In vivo admitivity measurements for regularizations in electrical impedance tomography

Sousa, T. H. S., samed.thais@gmail.com
Moura, F. S., fernandosmoura@gmail.com
Hoffmann, I. O., isadora.hoffmann@gmail.com
Camargo, E. D. L. B.,edlbcamargo@yahoo.com.br
Lima, R. G., lima.raul@gmail.com
Department of Mechanical Engineering - Polytechnic School of University of São Paulo, São Paulo, Brazil

H **Martins, A. R. C., doutorevet@hotmail.com**
Fantoni, D. T., dfantoni@usp.br
Biasi, C., caiobiasi@usp.br
Surgery Department - Faculty of Veterinary Medicine of University of São Paulo, São Paulo, Brazil

Abstract. *In this paper, in vivo measurement of tissues in beta dispersion region (0-200 kHz) was acquired. The measurements were carried out on suine tissue and constitute data for an anatomy and physiology based priors to be used as an Electrical Impedance Tomography regularization. Plunge electrodes in four-terminal configuration and a computer-automated measurement system were used to acquire admitivity data. Measurements were taken on myocardial muscle (three different positions on epicardial surface), pectoral and intercostal muscles, adipose tissue, cartilage and lung (cranial, medial and caudal lobe tissues). The admitivity measurements were carried in such way to allow anisotropy detection, at 125 kHz. Four animals were used for this experiment. Admitivity temporal variations synchronized with perfusion and ventilation rates were observed. Increased PEEP lead to increased time averaged admitivity in lung tissues.*

Keywords: Electrical impedance tomography, tissue admitivity, in vivo measurement, dielectric tissue properties

1. INTRODUCTION

Electrical Bioimpedance Monitoring is an emerging tool for biomedical research and for medical practice. It constitutes one of the diagnostic methods based on the study of the passive electrical properties of the biological tissues. The practical use of the electrical passive properties started in the middle of the XX century. Different properties and techniques resulted in a collection of methods that are now used for multiple applications. Usually, these methods have three advantages in common: require low-cost instrumentation; are easily applicable in practice; enable on-line monitoring. A review on applications of Bioimpedance methods can be found in Morucci *et al.* (1996).

Electrical Impedance Tomography (EIT) expands the usefulness of all this methods by adding spatial resolution. EIT provides a mapping of the impedance distribution in a tissue volume. Multiple electrodes are used to inject currents and record voltages. Reconstruction algorithms process the resulting data to generate an image. The spatial resolution is poor compared to other imaging methods (echography, X-ray tomography or Magnetic Nuclear Resonance) but its temporal resolution is good to monitor perfusion phenomena. It is sometimes justified in terms of cost, acquisition speed and information provided by the quantitative results.

In the EIT problem it can be identified a forward problem, which is to solve the electrode electric potentials corresponding to a given electrical current injection and impedance distribution within the domain, and an inverse problem, that is to find out the impedance distribution on the basis of the measured electrode electric potentials and imposed electrical currents. The inverse problem is a non-linear and ill-posed problem, that is, small measurement errors can cause large errors to the solution.

An ill-posed inverse problem achieve better solutions with the help of *a priori* information about the mathematical space of possible solutions. These information is used to regularize the inverse problem, restricting the solution space. One way to restrict the solution space is to use a statistical description of the solution space with clinically informative data (Kaipio and Somersalo, 2004). The statistical description of the solution space with clinical meaning is called an anatomy based prior. The main objective of this paper is to assemble a database of *in vivo* biological tissue admitivity values of the chest of pigs, which will contribute to an anatomy based prior for EIT.

2. MATERIALS AND METHODS

2.1 Measurement system

Our admitivity measurement device is composed by a probe with plunge electrodes, a sine wave generator fixed at 125 kHz which drives a voltage-to-current circuit and an acquisition board connected to a computer. The four-electrode

method was used in this study. This method has been commonly used in prior *in vitro* and *in vivo* tissue studies (Haemmerich *et al.*, 2002, 2003; Steendijk *et al.*, 1993; Tang *et al.*, 2008; Tsai *et al.*, 2000) because this configuration reduces errors due to polarization impedance and stray capacitances, according to Tsai *et al.* (2002). The needles have diameter $\phi =0.7$ mm and their positions are shown on Fig. 1 . The current source is connected to needle 1 and needle 4 is connected to ground through a resistor, with known resistance, which is used as sense resistor to compute the electrical current intensity and phase. Each acquisition board channel measures the potential between the respective needle and the ground.
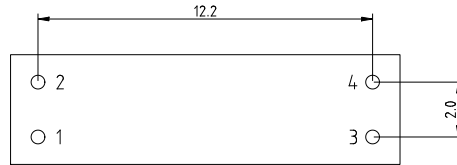

Figure 1. Probe main dimensions

2.2 Data acquisition and analysis

The acquisition board was set to an acquisition rate of 2.5 MHz for all channels, which gives 20 samples per sine period at 125 kHz. It was conceived to collect a set of 8000 samples of each channel (which needs 3.2 ms to be acquired) at every 0.05 s, during a period of 20 s to 25 s depending on the tissue.

After the data collection, each set of 8000 samples of each channel was used to adjust a sine wave at 125 kHz using a least mean square method to find its phasor representation. It was considered one *measurement*, the set of adjusted phasors of all four channels at a given time.

With the geometry of the problem given by needles position and the measurements acquired, one can solve the generalized Laplace Equation Eq. (1) for complex admitivity γ

$$\nabla\cdot(\gamma\nabla\psi) = 0, \tag{1}$$

where ψ is electrical potential inside the domain

This equation can be solved with the aid of a finite element method in a Newton-Raphson algorithm (Barber, 1989; Mello *et al.*, 2006). As hypothesis, it was assumed that in the neighborhood of the probe, γ is uniform, and the domain Ω is a half $\mathbb{R}^3$ space, truncated far enough from the needles so that this truncation do not influence the results. Figure 2.2 shows the mesh used on Newton-Raphson algorithm.
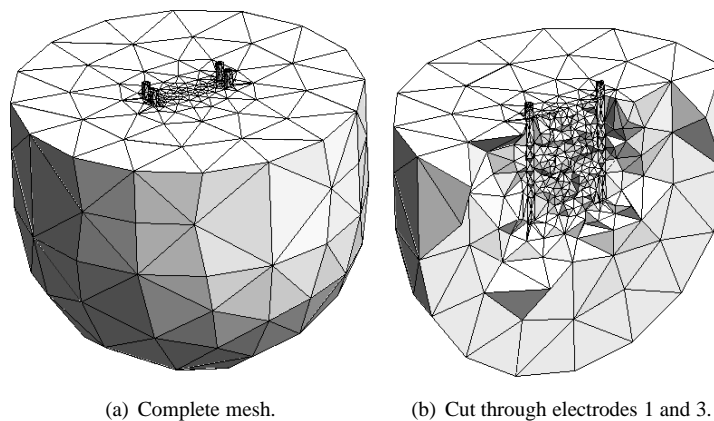
(a) Complete mesh.   (b) Cut through electrodes 1 and 3.

Figure 2. Finite element mesh.

In this method, only phasors V_2, V_3 on channels 2 and 3 are needed. The phasor V_4 on channel 4 is used only to compute the current $I = V_4/R$, where the sensing resistor value is known.

2.3 Experimental protocol

The protocol for this study was approved by the Animal Care and Use Committee Faculty of Veterinary Medicine University of São Paulo and was in compliance with all guidelines for the humane use of animals in research. Male and female pigs, four in total, weighing between 28 and 30 kg were selected. The experimental measurements were performed

on *in vivo* lungs, heart, adipose tissue, cartilage, pectoral and intercostal muscles. The measured points were chosen based on the anatomy of each organ and care was taken in order to avoid tissue damages.

A 5 mg/kg dose of Midazolam and 0.2 mg/kg dose of Ketamine intramuscularly. After fifteen minutes, and venous access established by puncturing the marginal ear vein to administer propofol at a dose 5 mg/kg intravenously. Intubation was instituted to maintain anesthesia with isoflurane inhalation (1.4%) in 70% oxygen. Neuromuscular blockade is performed by administering pancuronium 0.1 mg/kg. During the entire procedure will be performed fluid resuscitation with Ringer lactate at a rate of 2 mL/kg/h. Monitoring of anesthesia include measurement of blood pressure by invasive method, heart rate and respiratory rate, ventilator settings such as tidal volume and minute, peak pressure and mean arterial blood gases, oxygen saturation and bicarbonate as well as the assessment of carbon dioxide in exhaled air. At the end of the protocol the animal must be euthanized with administered sequentially 10 mL/kg of potassium chloride. The animals were placed on mechanical ventilator and maintained at a level near 100% oxygen saturation and the heart rate was kept between 90 and 120 bpm. The sternum was split by cutting from the xiphoid process through the most anterior aspect. The chest was held open by a surgical retractor exposing heart, lungs and muscles.

According to the organ, some specific directions were adopted. The probe was positioned on two distinctive directions to allow observing possible anisotropies. Table 1 summarizes the *in vivo* measurements locations and orientations.

Table 1. *in vivo* measurement locations

Location	Anatomical Orientation
Left lung, cranial lobe	Orientation 1: craniocaudal Orientation 2: laterolateral
Left lung, cranial lobe	Orientation 1: craniocaudal Orientation 2: laterolateral
Right lung, cranial lobe	Orientation 1: craniocaudal Orientation 2: laterolateral
Right lung, middle lobe	Orientation 1: craniocaudal Orientation 2: laterolateral
Right lung, caudal lobe	Orientation 1: craniocaudal Orientation 2: laterolateral
Heart	craniocaudal
Deep pectoral muscle	Orientation 1: longitudinal to fibers Orientation 2: transverse to fibers
Adipose tissue	tangential to ribs
Intercostal muscles	Orientation 1: longitudinal to fibers Orientation 2: transverse to fibers
Costal cartilage	No defined orientation

For lung measurements, three Positive End Expiratory Pressure (PEEP) were considered: 5, 10 and 15 mmHg, for all other tissues, PEEP was fixed at 5 mmHg.

3. RESULTS

Table 2 comprises the results obtained from the experiment. Both mean and standard deviation for admitivity and permittivity are shown for all tissues.

Table 2. *in vivo* admitivity results at 125 kHz

Tissue/location		PEEP (mmHg)	Orient./ Position	Conductivity ($\times \cdot 10^{-1}$ S/m)		Permittivity ($\times \cdot 10^{-8}$ F/m)	
				mean	st. dev.	mean	st. dev.
Left lung	Cranial lobe	5	1	2.82	2.75	3.58	2.49
			2	2.76	2.80	3.51	2.48
		10	1	2.75	2.82	3.57	2.67
			2	2.76	2.80	3.55	2.43
		15	1	2.74	2.85	3.56	2.81
			2	2.77	2.79	3.63	2.35
	Caudal lobe	5	1	3.24	2.67	3.36	2.66
			2	3.20	2.78	3.25	2.79
		10	1	1.96	1.40	3.76	2.47
			2	3.17	2.80	3.23	2.81
		15	1	3.09	2.74	3.28	2.75
			2	3.16	2.85	3.30	2.74
Right lung	Cranial lobe	5	1	2.75	2.81	4.14	2.47
			2	3.10	2.54	3.74	2.24
		10	1	2.73	2.83	2.03	1.61
			2	3.13	2.53	3.67	2.28
		15	1	1.49	0.857	3.75	2.64
			2	1.07	0.0332	3.62	2.42
	Middle lobe	5	1	2.71	2.80	3.45	2.22
			2	2.75	2.79	3.17	1.97
		10	1	2.65	2.83	3.22	2.34
			2	1.20	0.547	2.03	1.04
		15	1	2.62	2.85	3.08	2.30
			2	2.61	2.86	3.00	2.08
	Caudal lobe	5	1	3.37	2.54	5.21	3.02
			2	3.30	2.47	5.23	2.61
		10	1	3.31	2.54	5.06	2.72
			2	3.25	2.50	5.19	2.64
		15	1	3.23	2.58	4.53	2.44
			2	2.05	0.992	5.14	3.44
Heart		5	pos. 1	4.23	2.54	6.18	1.58
			pos. 2	4.39	1.87	6.27	0.675
			pos. 3	5.19	1.35	6.44	0.823
Muscles	Deep pectoral	5	1	4.76	1.58	11.3	5.60
			2	3.67	2.17	12.1	5.19
	Intercostal	5	1	4.90	1.34	7.48	4.94
			2	4.55	0.513	8.50	3.69
Adipose		5		2.01	0.819	5.46	3.86
Cartilage		5		7.29	1.59	2.23	2.66

4. DISCUSSION AND CONCLUSION

Due to muscles anatomy, the current density direction follows the arrangement of muscle fibers and the direction of insertion of the probe. The results show admitivity anisotropy, an expected characteristic of muscles.

From the results of the lungs, it can be seen that the electrical admitivity is smaller on the cranial lobes than on other parts. One hypothesis for this result is a greater amount of air in the cranial lobes, which would cause a decrease in admitivity. Increasing PEEP causes the admitivity to decrease in lung tissue. This effect is what allows us to estimate the amount of air in the lung tissue.

Cartilage data showed that the electrical admitivity is almost constant. One possible reason is the lack of vascularization of the cartilaginous tissue and no significant events occurred in this tissue, such as the increase of blood supply, which could cause a variation in admitivity. Adipose tissue shows some slight variations in electrical admitivity, consistent with the poor tissue perfusion.

The *in vivo* results presented here complements *in vitro* data reported in literature (Haemmerich *et al.*, 2002, 2003; Steendijk *et al.*, 1993; Tang *et al.*, 2008; Tsai *et al.*, 2000). From these experiments, it was possible to check the anisotropy of certain tissues, as well as the behavior of the electrical admitivity during the ventilation and perfusion cycles.

5. ACKNOWLEDGEMENTS

6. REFERENCES

Barber, D.C., 1989. "A review of image reconstruction techniques for electrical impedance tomography". *Medical Physics*, Vol. 16, pp. 162–169.

Haemmerich, D., Ozkan, R., Tungjitkusolmun, S., Tsai, J.Z., Mahvi, D.M., Staelin, S.T. and Webster, J.G., 2002. "Changes in electrical resistivity of swine liver after occlusion and postmortem". *Medical & Biological Engineering & Computing*, Vol. 40, pp. 29–33.

Haemmerich, D., Staelin, S.T., Tsai, J.Z., Tungjitkusolmun, S., Mahvi, D.M. and Webster, J.G., 2003. "In vivo electrical conductivity of hepatic tumours". *Physiological Measurement*, Vol. 24, pp. 251–260.

Kaipio, J. and Somersalo, E., 2004. *Statistical and Computational Inverse Problems*. Springer, New York, 1st edition.

Mello, L.A.M., Lima, C.R., Silva, E.C.N. and Lima, R.G., 2006. "Comparing two electrical impedance tomography algorithms: Gauss-newton and topology optimization". In *Proceedings of Medical Imaging 2006 - an SPIE event*. SPIE - The International Society for Optical Engineering, Bellingham.

Morucci, J., Valentinuzzi, M.E., Rigaud, B., Felice, C.J., Chauveau, N. and Marsili, P.M., 1996. "Biolectrical impedance techniques in medicine". *Critical Reviews in Biomedical Engineering*, Vol. 24, pp. 223–681.

Steendijk, P., Mur, G., Velde, E.T.V.D. and Baan, J., 1993. "The four-electrode resistivity technique in anisotropic media: theoretical analysis and application on myocardial tissue in vivo". *IEEE transactions on biomedical engeneering*, Vol. 40, pp. 1138–1148.

Tang, C., You, F., Cheng, G., Gao, D., Fu, F., Yang, G. and Dong, X., 2008. "Correlation between structure and resistivity variations of the live human skull". *IEEE transactions on biomedical engeneering*, Vol. 55, pp. 2286–2292.

Tsai, J.Z., Cao, H., Tungjitkusolmun, S., Woo, E.J., Vorperian, V.R. and Webster, J.G., 2000. "Dependence of apparent resistance of four-electrode probes on insertion depth". *IEEE transactions on biomedical engeneering*, Vol. 47, pp. 41–48.

Tsai, J.Z., Will, J.A., Stelle, S.H.V., Cao, H., Tungjitkusolmun, S., Choy, Y.B., Haemmerich, D., Vorperian, V.R. and Webster, J.G., 2002. "Error analysis of tissue resistivity measurement". *IEEE transactions on biomedical engeneering*, Vol. 49, pp. 484–494.

7. Responsibility notice

The authors are the only responsible for the printed material included in this paper.